Chapter 4

Silicon Heterojunction Solar Cells: The Key Role of Heterointerfaces and their Impact on the Performance

Miroslav Mikolášek

Additional information is available at the end of the chapter

http://dx.doi.org/10.5772/65020

Abstract

This chapter is dedicated to the processes linked with the collection of photo-generated carriers in silicon heterojunction (SHJ) solar cells with a focus on the key role of the amorphous silicon/crystalline silicon heterojunction. The intention is to explain the role of carrier inversion at the heterointerface and connect it with the properties of the SHJ to obtain deeper understanding of carrier transport properties and collection, which goes beyond amorphous silicon-based structures and will contribute to understanding the new emerging SHJ based on amorphous silicon oxide and metal oxide emitter layers. The study is extended by a simulation of the TCO/emitter interface with the aim to reveal the effect of parasitic Schottky barrier height on the performance of the SHJ solar cell. In addition, the simulation study of SHJ under concentrated light and varied temperatures is outlined to show the main limitations and prospects of SHJ structures for utilization under concentrated light.

Keywords: amorphous silicon, heterojunction, carrier inversion, open-circuit voltage, ASA simulation

1. Introduction

Among the semiconductor materials with suitable optoelectronic properties for photovoltaic applications, silicon has been the most widely accepted and used in the current production of photovoltaic modules. The basic advantage of silicon is its abundance in nature and mastered silicon wafer fabrication, as well as the compatibility of the technological processes of solar cells with the microelectronics industry. The increasing cost of processed crystalline silicon ingots in the past years became a driving force decreasing the wafer thickness for solar cell

fabrication [1]. However, this trend was stopped due to the bending of thin wafers during high temperature processing of standard silicon solar cells, which results into the increasing efforts focused on the technologies with lower silicon usage. Among them, the silicon heterojunction solar cells (SHJ) provide both high performance together with a perspective of low-cost fabrication and decrease of silicon wafers thickness bellow 100 μm [2]. The advantages of heterojunction between amorphous and crystalline silicon were first introduced into the so-called HIT concept (Hetero-junction with Intrinsic Thin-layer) by former company SANYO (currently SANYO is part of the company Panasonic) in 1992 [3]. The SHJ HIT solar cell is composed of a single thin crystalline silicon wafer, c-Si surrounded by ultra-thin intrinsic silicon layers, a-Si:H(i) and n-type and p-type doped amorphous silicon layers, a-Si:H (**Figure 1**), which can be deposited at temperature below 200°C and so can be used in processing of thin wafers. On the two doped layers, transparent conducting oxide (TCO) layers and metal electrodes are formed with sputtering and screen-printing methods, respectively. The TCO layer on the top also works as an anti-reflection layer.

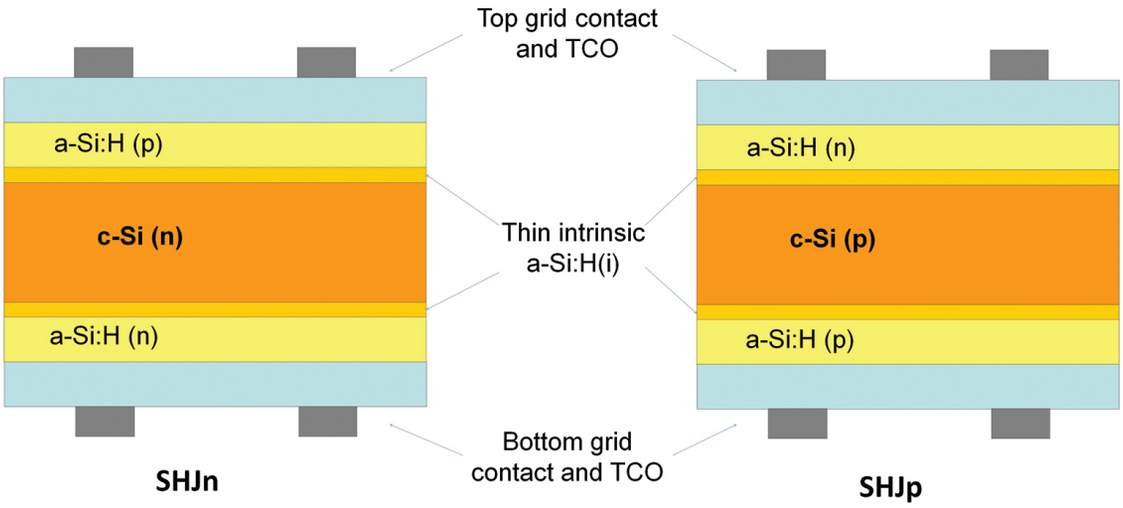

Figure 1. Silicon heterojunction solar cells with on n-type silicon (SHJn) and n-type silicon (SHJp) hetero-junction with intrinsic thin-layer (HIT) solar cell.

Since the first introduction, the HIT solar cells have been the subject of extensive research. Recently, the record efficiency η = 25.6% with open-circuit voltage V_{OC} = 0.74 V, short-circuit current J_{SC} = 41.8 mA/cm^2 and fill factor FF = 82.7% were achieved on the rear junction HIT solar cell by Panasonic, which makes this technology currently the most efficient among silicon-based solar cells [4]. Current strong interest in SHJ concept is motivated by the high conversion efficiency as well as further possibilities for decreasing the fabrication cost. SHJ can be prepared by simple and low temperature fabrication processes, which decreases the thermal budget and thus the cost of the cell. Since the base material of the structure is crystalline silicon, the typical degradation due to the Staebler-Wronski effect observed in amorphous silicon solar cells does not take place in SHJ solar cells, where the base material of the structure is crystalline silicon [5]. Moreover, the HIT cell shows a better temperature coefficient (<–0.25%/K) compared to standard c-Si solar cells (–0.45%/K), which means more power generated in outdoor conditions

for the same nominal conversion efficiency [6]. Since the SHJ HIT has symmetrical front and back structures, the possibility to use it for the bifacial solar module is feasible. The experiments show that bifacial use of the HIT structure brings a performance higher by more than 10% compared to the conventional structures with light incident only from one side [7].

1.1. Current trends in SHJ solar cell development

To make the SHJ solar cells more economically attractive, current efforts are focused on the development of technologies and approaches focused on two main objectives (i) to increase the efficiency and (ii) to decrease the fabrication costs. The utilization of emitters with a large band gap such as amorphous silicon carbide a-SiC:H [8], nanocrystalline silicon oxide nc-SiOx:H [9] or micro-crystalline silicon oxide μc-SiOx:H [10], thus lowering light absorption is a common approach on how to increase J_{SC} and hence the performance of such solar cells. The advantage of this approach is that only low adjustment of production lines is required for replacements of a-Si:H emitter by a-SiC:H or SiOx:H emitter layers. An increase in J_{SC} by about 1 mA/cm^2 was demonstrated by replacing a-Si:H by a-SiC:H [8] or by μc-SiOx:H [10]. However, also in this case the heterojunction with a c-Si substrate plays a crucial role and its fabrication has to be well mastered to benefit from the lower parasitic absorption of light. Another way on how to decrease absorption losses is based on the preparation of the two collection contacts at the bottom side of the silicon substrate forming an inter-digitated back contact silicon heterojunction (IBC-SHJ) solar cells. The beneficial effects of collection electrodes at the bottom of the cell are demonstrated by the best efficiency of 25.6% currently achieved at SHJ solar cells [4]. High J_{SC} = 41.8 mA/cm^2 in such solar cells is attained due to the eliminated absorption losses of a-Si:H layers as well as losses in TCO.

The decrease of fabrication cost can be realized through the replacement of expensive materials by cheaper alternatives. Several groups have investigated alternative materials such as zinc oxide, ZnO [11], and indium zinc oxide, IZO [12], as a replacement of expensive indium tin oxide, ITO. Replacement of silver used in the collection electrodes by copper [1, 13] is another way, and is currently highly investigated to decrease SHJ cost.

Another approach to make SHJ cells more economically attractive is based on the reduction of silicon wafer thickness. The ability of HIT structure to use silicon wafers of low thicknesses and to achieve high performance at the same time was demonstrated already in 2009, when the SHJ HIT solar cell with a conversion efficiency of 22.8% prepared on a 98 μm thick n-type silicon wafer was introduced by former company Sanyo (currently Panasonic) [2].

Nowadays, new advance concepts are emerging based on the replacement of the amorphous emitter by metal oxides [14–16]. Such a concept has the ability to provide both an increase of efficiency as well as a decrease of fabrication cost. Metal oxides provide advantages of large band gaps, thus lower parasitic absorption in the emitter, simpler deposition by thermal evaporation [13] and no requirements of toxic dopant gases during fabrication. Moreover, the deposition of such oxides can be carried out at low temperatures leading to a further decrease of the thermal budget and hence fabrication cost. Metal oxides are widely used as a hole transport layers in organic solar cells [16, 17]. Current attempts to transfer them into the SHJn technology show very promising results with achieved efficiency of η = 22.5% for

molybdenum oxide hole collector MoOx-based SHJ solar cell [18]. The progress in the development of electron selective contacts based on lithium fluoride (LiFx) allows fabrication of dopant-free asymmetric heterocontacts cell (DASH) with conversion efficiency approaching 20% [19].

1.2. Aim of this chapter

Two targets have to be attained for the good performance of solar cells: (i) light has to be absorbed in the absorption layer of the solar cell and (ii) the photo-generated carriers have to be effectively collected by the top and bottom collection electrodes. The first target is focused on the improvement of light management, which with the decreasing of the c-Si substrate thickness starts to be important also for SHJ solar cell. The optimization of TCO [12, 20], tuning of emitter layer band gap [8] and texturization of c-Si [21] are crucial to achieve high J_{SC}. The second target, which is described in detail in this chapter, is focused on the recombination and carrier transport processes in the structure. Such processes determine the collection of the photo-generated carriers and thus the performance of the solar cell. Since the SHJ is formed as a stack of various layers surrounding the absorber c-Si layer, the current transport of photo-generated electron/hole pairs to the collection electrodes is highly influenced by the interfaces between the neighbouring layers. Due to the connection of various materials with different lattice parameters, defect states can be formed at the interface. The difference in the band gap, affinity, doping level and type of adjacent layers results into the formation of heterojunctions/carrier transport barrier. Application of a-Si:H or alternative emitter (such as a-SiC:H, nc-SiOx or metal oxides) in the SHJ solar cell is linked with several challenging requests concerning the quality of this layer and its interfaces with c-Si and TCO. On the one hand, the defect states and band alignment at the a-Si:H/c-Si interface determine the band bending at the c-Si surface and hence recombination and collection of photo-generated carriers [6, 22, 23]. Good quality of the a-Si:H(i) layer as well as a-Si:H/c-Si interface is one of the main challenges in order to achieve high SHJ solar cell efficiency. On the other hand, due to the low specific conductivity of a-Si:H it is required to use conductive TCO as a collection electrode. When the TCO is not chosen carefully regarding the proper work function, or is not properly prepared, the parasitic Schottky barrier can arise at the TCO/a-Si:H interface [24–26]. This parasitic Schottky barrier has an opposite diffusion potential compared to the a-SiH/c-Si junction and thus hinders the collection of photo-generated carriers. As a result, the performance of the SHJ deteriorates.

The aim of this chapter is to explore the processes connected with the collection of photo-generated carriers and to explain the key role of the front a-Si:H/c-Si and TCO/a-Si:H interfaces for carrier recombination processes. ASA simulation is carried out to provide an insight into the charge properties of both a-Si:H/c-Si and TCO/a-Si:H junctions forming the front emitter stack of the SHJ solar cell and to explore their interconnection. Strong emphasis is focused on the presence of carrier inversion at the a-Si:H/c-Si, which is the most determining factor for V_{OC} of SHJ cell. The alternative approaches to obtain high carrier inversion based on field effect passivation and metal oxides are described in the chapter as well. The study is extended by simulation of the SHJ under concentrated light and varied temperatures to explore the

perspective and limitations of n- and p-type silicon-based SHJ structures for utilization in light concentrated applications.

1.3. Simulation set-up

The ASA simulation program was used for characterization of recombination processes in the SHJ structure. This program is designed for the simulation of solar cells based on a-Si:H and c-Si semiconductors. ASA program solves the Poisson equation and continuity equations for electrons and holes in one dimension and includes several physical models which describe the trapping and generation/recombination processes in the structures with consideration of spatial disorder of amorphous silicon [26]. The simulated solar cell structures have the following layer sequence: TCO/a-Si:H(n)/a-Si:H(i)/c-Si(p)/a-Si:H(i)/a-Si:H(p)/TCO/Metal and TCO/a-Si:H(p)/a-Si:H(i)/c-Si(n)/a-Si:H(i)/a-Si:H(n)/TCO/Metal denoted as SHJp and SHJn, respectively. In the simulated models, the thicknesses of 5 and 10 nm were used for a-Si:H(i) and doped a-Si:H(n) and a-Si:H(p) layers, respectively. The band gap of a-Si:H(p) was set to 1.95 eV and the band gaps of a-Si:H(i) and c-Si(n) were set to 1.76 eV in accordance to [27]. The doping activation energies of 0.2 and 0.4 eV were used for a-Si:H(n) and a-Si:H(p) layers, respectively. The gap state densities of amorphous layers have a Gaussian distribution of dangling bonds and an exponential distribution of band tails was set together with additional parameters according to the literature [27]. While the main aim of the simulation is to describe recombination processes in the structure, flat silicon substrate conditions were used in the models. The silicon substrates with thickness of 200 μm, lifetime, τ = 1 ms and concentration of dopants, $N_{dop} = 5 \times 10^{21}$ m^{-3} were used for both SHJp and SHJn structures. TCO was adopted as an optical layer with a thickness of 80 nm. The defect states at the front a-Si:H/c-Si interface was modelled by inserted 1 nm thick highly defective c-Si layer. Flat band conditions at the TCO/a-Si:H interface were used in the initial simulations focused on the study of a-Si:H/c-Si properties. The negligible defect state density of 10^9 cm^{-2} were set at the back c-Si/a-Si:H contact for all simulations. The conduction band offset, $\Delta E_C = 0.15$ eV, and valence band offset, $\Delta E_V = 0.55$ eV, were used as an initial values determining band alignments in SHJp and SHJn structures, respectively. As an illumination source the light with power density of 100 mW/cm^2 and spectrum AM1.5 was used for the output performance simulations.

2. Open circuit voltage and carrier inversion

The output performance of the solar cells can be described by V_{OC}, J_{SC} and FF. All such parameters are linked with the η and define the overall output performance of solar cells. While the main aim of this chapter is to describe the role of heterointerface and inversion at the a-Si:H/c-Si, we will focus on V_{OC} which is strongly affected by recombination properties and carrier transport in the solar cell. The V_{OC} for SHJp solar cells can be expressed by the analytical model as [28, 29]

$$V_{\mathrm{OC}} = \frac{E_{g-Si} - \delta_{Si(p)}}{q} - \frac{kT}{q} \ln \left(\frac{N_C}{\Delta n} . \frac{\frac{D_\mathrm{p}}{L_\mathrm{p}} + S_\mathrm{p}}{\frac{D_\mathrm{p}}{L_\mathrm{p}}} \right) \tag{1}$$

Similarly for SHJn, the V_{OC} is expressed as

$$V_{\mathrm{OC}} = \frac{E_{g-Si} - \delta_{Si(n)}}{q} - \frac{kT}{q} \ln \left(\frac{N_V}{\Delta p} . \frac{\frac{D_\mathrm{n}}{L_\mathrm{n}} + S_\mathrm{n}}{\frac{D_\mathrm{n}}{L_\mathrm{n}}} \right) \tag{2}$$

Symbols in the above equations denote: T is the temperature, q is the elementary charge, k is the Boltzmann constant, $E_{\mathrm{g\text{-}Si}}$ is the band gap of c-Si, N_C and N_V are the effective densities of states in the conduction band of c-Si, $\delta_{Si(p)}$ and $\delta_{Si(n)}$ are the dopant activation energies of c-Si substrate with p-type and n-type doping, respectively, L_p and L_n are diffusion lengths for holes and electrons, respectively, and D_p and D_n are diffusion constants for holes and electrons. Further symbols denote the interface recombination velocities for holes $S_\mathrm{p} = C_\mathrm{p} D_\mathrm{it}$ and electrons $S_\mathrm{n} = C_\mathrm{n} D_\mathrm{it}$, where C_p and C_n are the capture rate coefficients for holes and electrons, respectively, and D_it is the interface defect density. The $\Delta p = \Delta n = g \,.\, \tau_{\mathrm{eff}}$ in the equations denotes the excess carrier concentration, where g is the average photo-generation of the electron-hole pairs in c-Si and τ_{eff} is the effective lifetime of the excess carries.

From the above equations it is apparent that V_{OC} depends on Δn, which is determined by τ_{eff} and g. g is related with the illumination intensity. τ_{eff} is determined by the recombination velocities S_p and S_n and thus by the defect state density at the a-Si:H/c-Si heterointerface, D_it recombination at the rear surface and recombination in the c-Si substrate. The recombination in the c-Si substrate is not the subject of this chapter, instead of this, we focus our attention to the a-Si:H/c-Si interface and inversion layer formed at c-Si surface of this interface. In the case of low recombination in the bulk and at the back surface of c-Si, the main recombination path is at the heterointerface. For such a case, the saturation current of the SHJ, J_{sat}, is determined by the saturation current of interface recombination $J_{\mathrm{sat\text{-}it}}$, which is for SHJp determined by the interface recombination velocity S_n and holes concentration at the heterointerface p_{it} as

$$j_{\mathrm{sat-it}} = q S_\mathrm{p} p_{\mathrm{it}} \tag{3}$$

Similarly, by considering interface concentration of electrons n_{it} for SHJn it can be written

$$j_{\mathrm{sat-it}} = q S_\mathrm{n} n_{\mathrm{it}} \tag{4}$$

By taking into account the equation for V_{OC}

$$V_{OC} = \frac{AkT}{q} \ln\left(\frac{j_{SC}}{j_{sat}}\right) \tag{5}$$

and substituting $J_{sat\text{-}it}$ as a saturation current, it is possible to write equation which determines the V_{OC} as a function of the interface recombination velocity and effective barrier for recombination at the heterointerface Φ_B [30]

$$V_{OC} = \frac{\Phi_B}{q} - \frac{AkT}{q} \ln\left(\frac{qN_V S_p}{j_{SC}}\right) \tag{6}$$

for SHJp and

$$V_{OC} = \frac{\Phi_B}{q} - \frac{AkT}{q} \ln\left(\frac{qN_C S_n}{j_{SC}}\right) \tag{7}$$

for SHJn, where A represents the diode ideality factor. From the above equation it is obvious that V_{OC} is determined by the Φ_B which should have a high value to obtain high V_{OC}. **Figure 2** show the band diagram of SHJn and SHJp with Φ_B at the heterointerfaces, respectively. In SHJ solar cells the c-Si surface at the heterointerface is inverted or strongly inverted, forming an inversion layer with a high concentration of minority carriers [31, 32] at the heterointerface. From the band diagram, the rate of the inversion is determined by the bending of bands at the surface of c-Si and can be expressed as a distance of the Fermi level from the conduction band level at the heterointerface, $E_i = E_C - E_f$. It is obvious that the car-

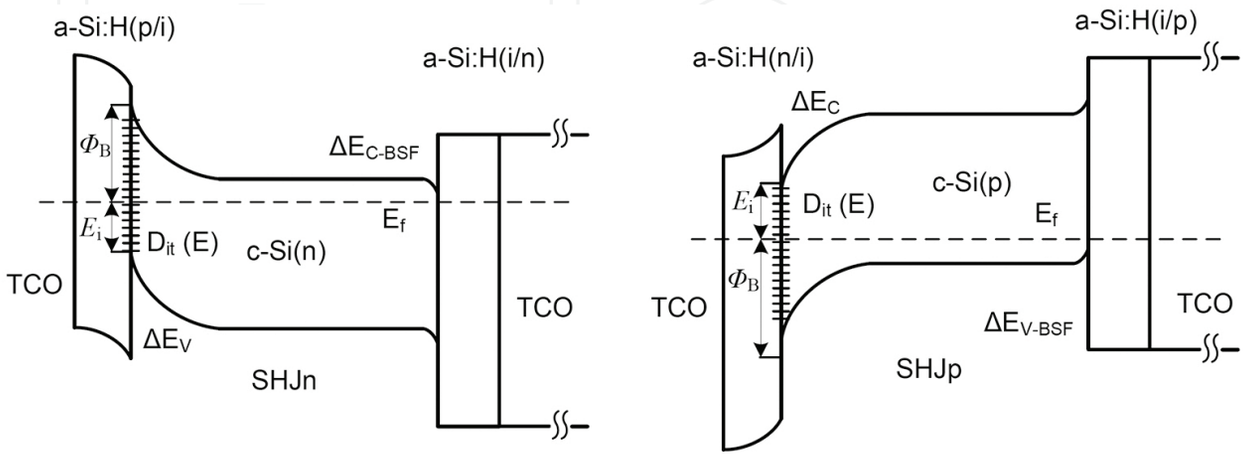

Figure 2. Band diagram of (left) SHJn and (right) SHJp structures with sketched barrier for interface recombination Φ_B at interface defects D_{it}.

rier inversion is linked with Φ_B thus directly related to V_{OC}. For both SHJ, high carrier inversion is required to obtain high value of Φ_B and thus high V_{OC}. Eqs. (1) and (2) do not take into account the influence of a-Si:H layer and indicate that V_{OC} depends on the illumination intensity, recombination properties at the heterointerface, recombination at the rear surface and in the c-Si substrate, and on the dopant activation energy of the c-Si substrate. The properties of the emitter seem to play no role in the V_{OC}. In fact, the parameters like doping, defect density and affinity (or band offset with c-Si) have no direct influence on the V_{OC}. However, all of these parameters affect the charge properties of the space charge region (SCR) of SHJ junction and thus carrier inversion at the heterointerface and consequently V_{OC}. In the following sections, we will describe by means of simulation various SHJ solar cell properties which affect carrier inversion and V_{OC}.

3. Front a-Si:H/c-Si heterointerface

3.1. Front a-Si:H/c-Si: influence of interface defect states

The front a-Si:H/c-Si heterointerface is a key part of the SHJ solar cell which has the main influence on the recombination processes in the structure and thus the output performance. The connection of two materials with different band gaps, lattice and electrical properties results into the formation of band discontinuity and defect states at the interface. Such properties are strongly affecting the carrier transport through that interface. In order to investigate the influence of D_{it} on the carrier inversion and hence recombination activity at the interface, numerical calculations using the program ASA was carried out. **Figure 3(a)** shows V_{OC} and η calculated as a function of D_{it} for SHJp and SHJn solar cell structures. As can be seen, V_{OC} and hence η exhibit a decrease upon the increase of D_{it} for both SHJp and SHJn structures. To explain the recombination processes at the a-Si:H/c-Si interfaces connected with the presence of defect states, it is necessary to consider the band diagram. Analysis will be provided for SHJp structure, however, conclusions are applicable also to SHJn structure. **Figure 3(b)** shows the band diagram of SHJp structure calculated for two values of D_{it}. In the case of SHJp structure with negligibly low $D_{it} = 10^9$ cm^{-2}, the rectification behaviour of the junction is formed due to the presence of the negative and positive space charges in the space charge region (SCR) of the c-Si and a-Si:H part of the junction, respectively. The SHJ solar structure exhibits a high asymmetry of doping, which shifts the SCR into the c-Si part of the junction, leaving a negligible part of the diffusion voltage V_d in the a-Si:H. Due to the presence of band discontinuity in the SHJp solar cell structure, the bands in the c-Si bend downwards and a high concentration of minority electrons is formed at the c-Si surface at the a-Si:H/c-Si interface. Such a layer with a high concentration of minority carriers is called an inversion layer. In the case of high inversion, the concentration of minority electrons is high and the concentration of majority holes is low at the c-Si surface of the heterointerface. For SHJp structure, the photo-generated electrons are collected by the front electrode and transferred through the front heterointerface. High carrier inversion and thus a low concentration of holes results into a low probability of photo-generated electrons to recombine with them. Such a behaviour is characterized by the barrier for interface recombination Φ_B, which is for SHJp

expressed by Eq. (6). The high carrier inversion, in other words high value of Φ_B, leads to low interface recombination. From this it is obvious that carrier inversion plays a crucial role in the V_{OC} of SHJ solar cell. The carrier inversion is changed by introducing a high value of defect states at the interface, $D_{it} = 6 \times 10^{12}$ cm^{-2}. Such defect states affect the charge conditions in the SCR of junction. The defects states at the heterointerface represent traps which are for SHJp structure occupied by electrons forming negative charge Q_i in the SCR at the c-Si part of the junction. Such negative Q_i screens the positive charge in the a-Si:H part of the junction and thus hinders the extension of the SCR in the c-Si. As results, the band bending and electric field in the c-Si part of the junction are lowered, which decreases the carrier inversion at the interface and causes decrease of Φ_B followed by an increase of interfacial recombination. Moreover, due to the lower electric field, the majority of holes have a high probability to diffuse to the interface and contribute to the recombination at the interface [28]. The same mechanism of carrier inversion decrease caused by the presence of Q_i is presented in case of SHJn solar cells (not shown here). However, due to the n-type silicon used in SHJn solar cells and holes collected through the front contact, the Q_i has a positive charge. Comparing both structures (**Figure 3a**), the SHJn structure exhibits a lower sensitivity to D_{it} and a higher efficiency. There are two main sources of such a higher efficiency for the SHJn structure. The first source is the higher FF (not shown here) of SHJn structure compared to SHJp structure. The second reason is the collection of holes through the front heterointerface of SHJn structure, which due to the band alignment exhibits lower interface recombination. The impact of the band alignment on the carrier inversion of SHJ structures is further discussed in Section 3.2.

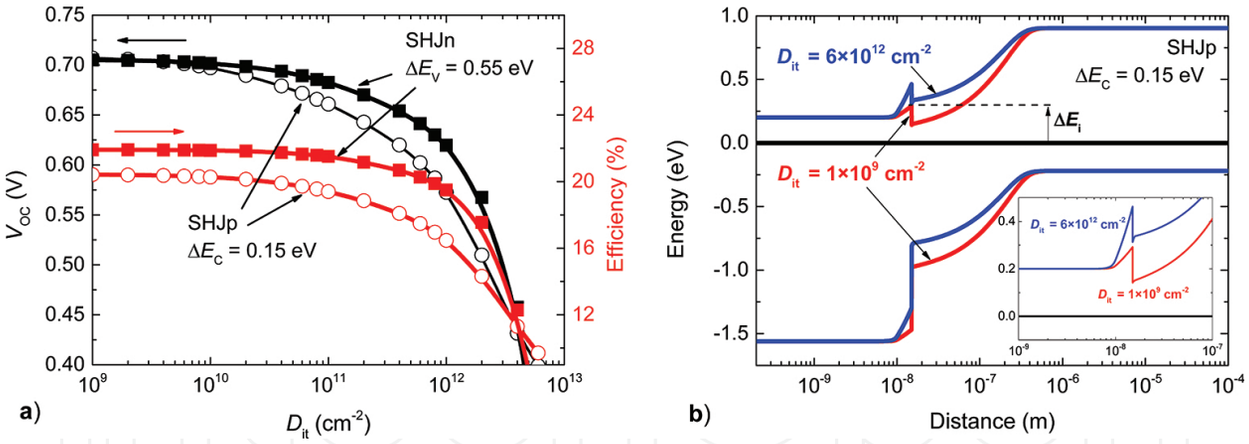

Figure 3. (a) The V_{OC} and η calculated in dependence on D_{it} for SHJn and SHJp structures. (b) Band diagrams calculated for two values of D_{it} for SHJp structure. The inset shows the change of carrier inversion (change in the distance of the conduction band level from the Fermi level at the heterointerface) with the change of D_{it}.

From the above discussion it is clear that the change of the charge properties in the SCR plays the key role for the carrier inversion at the heterointerface and strongly affects V_{OC}. The D_{it} are formed by acceptor and donor types of defects which form negative and positive charges in the c-Si part of SCR, respectively. Our recent study shows that the band bending at the c-Si part of the structure is lowered mainly due to the presence of Q_i with negative charge and Q_i with positive charge for SHJp and SHJn solar cells, respectively [22]. Because of this, the defect

asymmetry at the interface plays also an important role for the recombination processes at the interface [22]. The presence of acceptor defects at the heterointerface is more detrimental for the function of SHJn, while in the case of SHJp structure the donor defects are more affecting the performance of solar cell.

3.2. Front a-Si:H/c-Si: influence of band alignment

Comparing with the standard c-Si-based solar cells, the SHJs are characterized by the formation of a carrier inversion layer of minority carriers at the c-Si surface. The origin of this inversion layer steams from the presence of the band discontinuity at the interface and is the main factor for higher V_{OC} compared to the standard c-Si-based solar cells. In order to describe the impact of band alignment on the V_{OC}, simulation of SHJp solar cells with a varied conduction band offset ΔE_C is presented in **Figure 4(a)**. The impact of non-ideal a-Si:H/c-Si interface is shown as well by using four different values of D_{it}. Clearly, the decrease of ΔE_C results in the decreases of V_{OC}. This effect is stronger, when higher D_{it} is present at the interface. On the other hand, for high ΔE_C, the D_{it} has a weaker impact on the V_{OC}. Such a behaviour can be explained by considering the band bending and carrier inversion in the structure. **Figure 4(b)** shows band diagrams of SHJp solar cells for $D_{it} = 5 \times 10^{11}$ cm^{-2} and two values of ΔE_C. As can be seen, higher ΔE_C results into higher band banding in the c-Si part of the junction and stronger carrier inversion at the heterointerface. Because of this, V_{OC} exhibits higher values for structures with high ΔE_C. Moreover, the strong inversion causes a pronounced suppression of interface recombination since only few majority carries are available for recombination. As a result, the negative impact of D_{it} is less serious for structures with high values of ΔE_C. From this it is obvious that the ability to prepare a-Si:H/c-Si with high ΔE_C should be the way how to suppress the influence of D_{it} and how to attain high V_{OC} and thus the efficiency of SHJ solar cells. However, there are only limited possibilities to modify the band alignment of a-Si:H/c-Si heterointerface based on tuning the hydrogen content in the a-Si:H layer [33]. The literature presents a consensus that ΔE_C at a-Si:H(n)/c-Si(p) heterointerface is below 0.30 eV [23, 34–36].

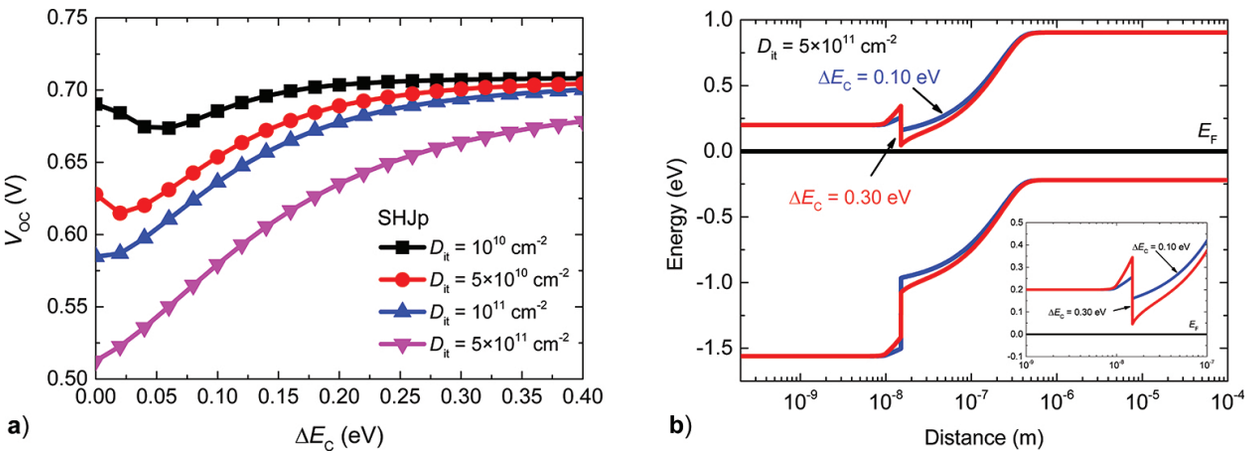

Figure 4. (a) V_{OC} calculated as a function of ΔE_C at the front a-Si:H/c-Si of SHJp solar cell structure. D_{it} is varied as a parameter in the simulations. (b) Band diagrams calculated for two values of ΔE_C and $D_{it} = 5 \times 10^{11}$ cm^{-2} of SHJp solar cell structure. The inset shows the change in the carrier inversion (change in the distance of the conduction band level from the Fermi level at the heterointerface).

Therefore, the critical aspect to obtain high V_{OC} of SHJ structures remains the suppression of defect states at the interface.

In the case of the SHJn structure, the transport of photo-generated minority holes is affected by the valence band offset ΔE_V which, due to the band alignment, has a higher value compared to the ΔE_C of SHJp. Because of this, the SHJn solar cell structures have higher carrier inversion at the interface as well as higher Φ_B and exhibit higher V_{OC} compared to the SHJp structures. Moreover, due to the higher carrier inversion the SHJn structure exhibits a lower sensitivity to D_{it} compared to the SHJp structure (**Figure 3a**).

3.3. Front a-Si:H/c-Si: influence of a-Si:H(i) passivation layer

The most straightforward way to increase the carrier inversion at the c-Si surface is to decrease D_{it}. The a-Si:H emitter with p- or n-type doping is characterized by a high concentration of defects resulting in a high D_{it} at the a-Si:H/c-Si interface. Because of this a thin intrinsic passivation layer of a-Si:H(i) with a significantly lower defect concentration ~5×10^{21} m^{-3} [36] compared to doped a-Si:H layer [27] is inserted at the interface. The quality of the a-Si:H(i) and thus passivation effect increases with the increase of a-Si:H(i) thickness $d_{a\text{-Si:H(i)}}$. However, high $d_{a\text{-Si:H(i)}}$ results in a decrease of FF and performance of SHJ solar cell [37].

A simulation study with a-Si:H(i) inserted at the heterointerface was carried out to describe the impact of $d_{a\text{-Si:H(i)}}$ on the carrier inversion at the c-Si surface and consequently on V_{OC} and the output performance. **Figure 5(a)** shows V_{OC} simulated as a function of $d_{a\text{-Si:H(i)}}$. Three values of D_{it} were used in the simulation as a parameter reflecting the possible passivation effect of a-Si:H(i) layer. In the case of low $D_{it} = 10^9$ cm^{-2}, the change of V_{OC} with $d_{a\text{-Si:H(i)}}$ is negligible. On the other hand, for higher value of D_{it} the decrease of V_{OC} with increase in $d_{a\text{-Si:H(i)}}$ is more relevant. V_{OC} is less sensitive to the presence of D_{it} for low $d_{a\text{-Si:H(i)}}$. This sensitivity to D_{it} increases with increasing $d_{a\text{-Si:H(i)}}$. The band diagrams for $D_{it} = 5 \times 10^{11}$ cm^{-2} and with $d_{a\text{-Si:H(i)}}$ of 10 and 50 nm were calculated to explain the impact of $d_{a\text{-Si:H(i)}}$ on V_{OC} at high D_{it} (**Figure 5b**). The band lines of a-Si:H(i) were aligned for both thicknesses to have the heterointerface at the same place. **Figure 5(b)** shows the decreases of band bending in the c-Si, thus the decrease of the carrier inversion at the heterointerface upon the increase of $d_{a\text{-Si:H(i)}}$ for $D_{it} = 5 \times 10^{11}$ cm^{-2} resulting in the decreases of V_{OC}. The a-Si:H(i) layer has a low concentration of free carriers and thus is a source of a potential drop across this layer, which affects the charge distribution and electric field in the SCR. This potential drop increases with the increase of $d_{a\text{-Si:H(i)}}$. In the case of low $D_{it} = 10^9$ cm^{-2} the strong carrier inversion occurs, in other words a high minority carrier concentration at the c-Si surface screens the potential drop over the a-Si:H(i) layer. Consequently, the potential drop over the a-Si:H(i) layer has a negligible influence on the carrier inversion and thus causes a negligible change of V_{OC} even at high $d_{a\text{-Si:H(i)}}$. In the case of high $D_{it} = 5 \times 10^{11}$ cm^{-2} the carrier inversion is much weaker due to the presence of trapped charge Q_i. Such trapped charge lowers the electric field in the c-Si, hence lowers band bending and decreases the carrier inversion at the c-Si surface. Due to the high Q_i the higher concentration of localized charge in the a-Si:H part of the junction is required to screen the charge in the c-Si. Because of this the potential drop over the a-Si:H(i) becomes more important for the distribution of the diffusion potential in the junction and with an increase of the $d_{a\text{-Si:H(i)}}$ the SCR is more widened

in the amorphous emitter (formed by the intrinsic and doped parts) resulting in an increase of the diffusion voltage in a-Si:H part of the junction and in a decrease of carrier inversion at c-Si surface of the a-Si:H/c-Si interface with increased $d_{a\text{-}Si:H(i)}$. This conclusion is in accordance with experimental observation [38]. V_{OC} decreases as a consequence of weaker carrier inversion. In accordance with this explanation, **Figure 5(b)** shows a more significant decrease of band banding in the c-Si and an increase of the band banding in the a-Si:H followed by a decrease of the carrier inversion at the interface for $d_{a\text{-}Si:H(i)}$ = 50 nm compared to the sample with $d_{a\text{-}Si:H(i)}$ = 10 nm. While the quality and thus passivation properties of the a-Si:H(i) layer increase with the thickness, careful tuning of the thickness and passivation ability is required to achieve high V_{OC} and high output performance. The same principle can be applied to the SHJn structure.

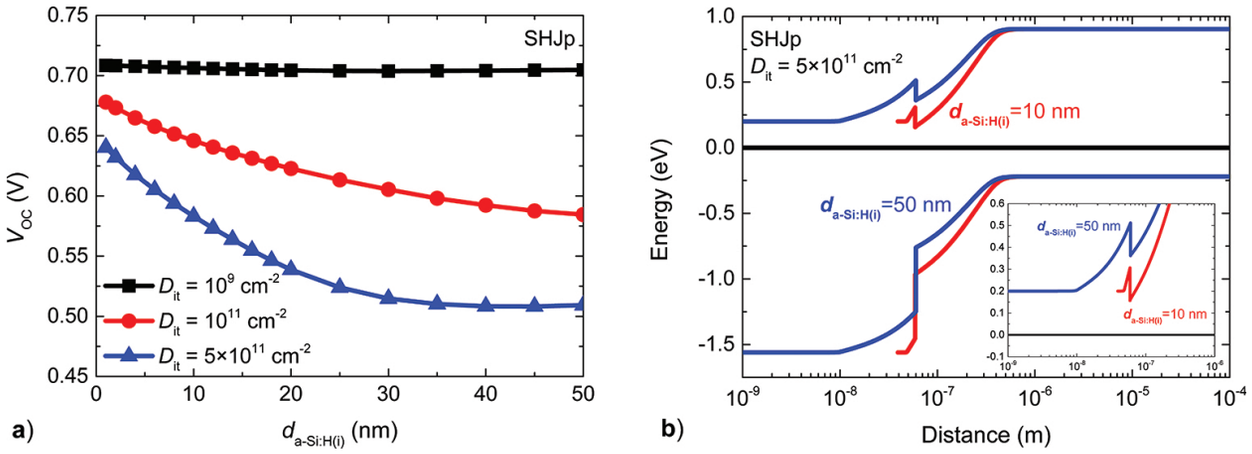

Figure 5. (a) V_{OC} calculated as a function of a-Si:H(i) thickness, $d_{a\text{-}Si:H(i)}$ inserted at the front a-Si:H/c-Si of SHJp solar cell structure. D_{it} is varied as a parameter in the simulations. (b) Band diagrams calculated for two values of $d_{a\text{-}Si:H(i)}$ and D_{it} = 5 × 10^{11} cm^{-2} for SHJp solar cell structure. The inset shows the change in the carrier inversion (change in the distance of the conduction band level from the Fermi level at the heterointerface).

3.4. Alternative concepts to obtain carrier inversion at emitter/c-Si interface

From the above discussion it is clear that high carrier inversion at the emitter/c-Si interface is crucial for high V_{OC} and high output performance of the SHJ solar cell. The high carrier inversion in the SHJ solar cells can be attained through (i) modification of band alignment at the heterointerface or (ii) by a decrease of D_{it} by optimizing the cleaning process or by insertion of a thin passivation a-Si:H(i) layer [6]. In following, we will discuss two alternative concepts of emitters which allow formation of high inversion at the emitter/c-Si interface and offer perspective to achieve high performance. The first one is the hetero-homojunction concept based on the field passivation effect [39, 40] and the second one is the use of alternative emitters based on transition metal oxides TMO with high W_f, which form the hole transport layers in SHJn structures [41].

The first alternative approach is based on the insertion of a highly doped c-Si layer of n^+- and p^+-type doping at the a-Si:H/c-Si interface of SHJp and SHJn solar structure, respectively [39, 40]. Such a highly doped layer with opposite doping of c-Si provides field passivation, and causes a shift of the Fermi level, which leads to an increase in carrier inversion at the c-Si surface. Our recent simulation study shows that by using the field effect passivation it is possible to decrease the sensitivity of V_{OC} to D_{it} and ΔE_C at the a-Si:H/c-Si interface [40]. The main drawback of this approach is, however, the additional technological steps required for preparation of a thin highly doped c-Si layer [42].

TMO with a high work function W_f such as MoOx, V_2O_5 and WO_3 represent alternative materials which can replace the a-Si:H emitter and can provide high carrier inversion at the c-Si surface [41]. The work function of these oxides changes according to the presence of adjacent environment or layer and varies in the range from 6 to 7 eV for as deposited layers and from 5 to 5.3 eV for oxides exposed to air [41]. Due to the intrinsic oxygen vacancies in their structure TMO are acting as n-type semiconductors [41, 43]. However, due to the high W_f TMO provides band alignment with c-Si in the way that acts as a p-contact and allows formation of a depletion silicon surface and strong carrier inversion at the interface in connection with n-type c-Si. Also in the case of SHJ with TMO, the carrier inversion is strongly affected by the defect states at the heterointerface, thus passivation a-Si:H(i) layer is required to insert at the TMO/c-Si interface to provide high performance of such SHJ solar cell structures. The efficiency of 22.5% was obtained for MoOx based on SHJ cell [18]. Despite the high efficiency obtained on TMO-based SHJ, the carrier transport mechanism and collection of photo-generated carriers are still not fully understood. Recent results suggest that regardless of the rectification behaviour caused by the high W_f, classical depletion approximation can be used to describe the rectification behaviour of TMO/c-Si junction [41]. It was shown that measured *I-V* curves can be described by a two-diode model with current transport limited by the recombination in the SCR of c-Si and diffusion of injected minority carriers [41]. However, further research is required to understand the extraction mechanism of photo-generated holes assisted by the gap states in the emitter based on the metal oxide.

4. Front TCO/a-Si:H heterointerface

4.1. Front TCO/a-Si:H: impact of parasitic Schottky barrier

The above simulation study revealed that V_{OC} is strongly determined by the properties at the front a-Si:H/c-Si heterointerface. Defect states and band alignment affect the distribution of the charge in the SCR and thus directly influence the electric field and carrier inversion at the heterointerface. The photo-generated carriers are collected by the front TCO and metal contacts. While TCO can be considered as a degenerated semiconductor, the properties at TCO/a-Si:H have to be also considered for carrier transport [44–46]. The most critical aspect for carrier transport is the possible presence of a parasitic Schottky barrier at the TCO/a-Si:H interface which can arise due to an inappropriate work function of TCO, W_{TCO} [24]. W_{TCO} depends on the material used as a TCO as well as on the deposition conditions used for

preparation. For example, in the case of ITO work functions of 4.2–5.3 eV were reported [45, 47]. The most common way to modify W_{TCO} is by controlling the oxygen pressure or pre- and post-deposition annealing [46]. It was shown that the parasitic Schottky barrier at TCO/a-Si:H interface of value Φ_{TCO} = 0.35 eV can reduce the conversion efficiency by more than 40% due to the deteriorated light current-voltage characteristics, which follows the so-called S-shape [48]. The Φ_{TCO} is partially affected by the carrier doping in the TCO layer, which shifts the Fermi level and thus affects the band alignment at the TCO/a-Si:H. Depending on the magnitude of Φ_{TCO}, different carrier transport mechanisms should provide a good contact TCO/a-Si:H. In the case of low Φ_{TCO}, thermionic emission should take place as a dominant transport mechanism of carriers. In the case of high Φ_{TCO}, tunnelling should take place to assist in the carrier transport. For tunnelling to be active it is necessary to have a high doping at both adjacent parts of the junction [46]. Recently, it was shown that high doping of TCO can result in lowering of the passivation and thus decrease the carrier inversion at the a-Si:H/c-Si, resulting in a decrease of V_{OC} and output performance [46]. Because of this, it is necessary to carefully consider not only the W_{TCO} but also the appropriate carrier doping to achieve a loss-free TCO/a-Si:H interface.

In the following simulation, the TCO is considered as a metal contact and the impact is simulated of low parasitic Φ_{TCO} at the TCO/a-Si:H emitter on the performance of SHJp solar cell. The aim of this simulation is to describe the impact of the Φ_{TCO} on the carrier inversion at the a-Si:H/c-Si of SHJp solar cells with conclusions which can be extended to the SHJn solar cell. **Figure 6(a)** shows V_{OC} simulated as a function of emitter layer thickness d_{emitt} and as a function of Φ_{TCO}. To model the high and low quality of a-Si:H/c-Si interface, two values of negligible low D_{it} = 10^9 and high 5 × 10^{11} cm^{-2} were adopted in the simulations. For the low value of D_{it} a negligible change of V_{OC} with Φ_{TCO} is observed. On the other hand, the change of V_{OC} with Φ_{TCO} is more relevant for high values of D_{it}. With the increase of d_{emitt} the influence of Φ_{TCO} on V_{OC} becomes negligible. Φ_{TCO} has an impact only on SHJp with a high value of D_{it} and low d_{emitt}. To explain such a behaviour, **Figure 6(b)** shows the band diagrams of SHJp structures with Φ_{TCO} = 0.2 eV, D_{it} = 5 × 10^{11} cm^{-2} simulated for d_{emitt} = 1 and 8 nm. For comparison reasons, the band diagram of SHJp with d_{emitt} = 8 nm and without parasitic Schottky barrier is shown as well. The band lines for both d_{emitt} were aligned to have the heterointerface at the same distance. As can be seen, the structures with Φ_{TCO} = 0 eV and Φ_{TCO} = 0.2 eV simulated with d_{emitt} = 8 nm exhibit the same carrier inversion at the silicon surface of the a-Si:H/c-Si interface. The carrier inversion is, however, significantly lowered when d_{emitt} decreases to 1 nm. The parasitic Φ_{TCO} forms SCR at the TCO/a-Si:H contact and thus is the source of an electric field with opposite direction to the electric field at the a-Si:H/c-Si junction. In the case of low D_{it} the strong carrier inversion at the c-Si surface of a-Si:H/c-Si interface screens the charge and electric field in the SCR of Φ_{TCO}. As a result, Φ_{TCO} has only a negligible impact on the band bending as well as on the carrier inversion and V_{OC} (**Figure 6b**). For D_{it} = 5 × 10^{11} cm^{-2} the carrier inversion at the a-Si:H/c-Si is significantly lowered due to the presence of Q_i. For such conditions, the distribution of the electric field in the a-Si:H emitter is more sensitive to $\Phi_{TCO.}$ In case of high d_{emitt}, the free carriers in the emitter can screen the impact of Φ_{TCO} and the electric field formed in the SCR of Φ_{TCO} barrier, thus no relevant decrease of carrier inversion at a-Si:H/c-Si is observed. With a decrease of d_{emitt} the SCR of

http://dx.doi.org/10.5772/65020

Φ_{TCO} can reach the SCR of SHJp. For such a case, the electric field of Φ_{TCO} lowers the diffusion potential of a-Si:H/c-Si and the parasitic Schottky barrier attracts the holes from the c-Si. As a result, carrier inversion at the interface decreases, leading into a decrease of V_{OC} and thus the overall performance decreases. Simulation results revealed that the negative influence of the parasiticΦ_{TCO} is due to the change of the carrier inversion at the a-Si:H/c-Si interface caused by the electric field of SCR at TCO/a-Si:H contact. Such a change is, however, possible only for low emitter thicknesses which have not sufficient charge for screening of Φ_{TCO}. Obviously, the doping of the emitter layer, in other words, the concentration of free carriers will also affect the screening ability of the emitter. With decrease of the doping, Φ_{TCO} will have more significant impact on the carrier inversion at the a-Si:H/c-Si interface and thus will more rapidly deteriorate the output performance.

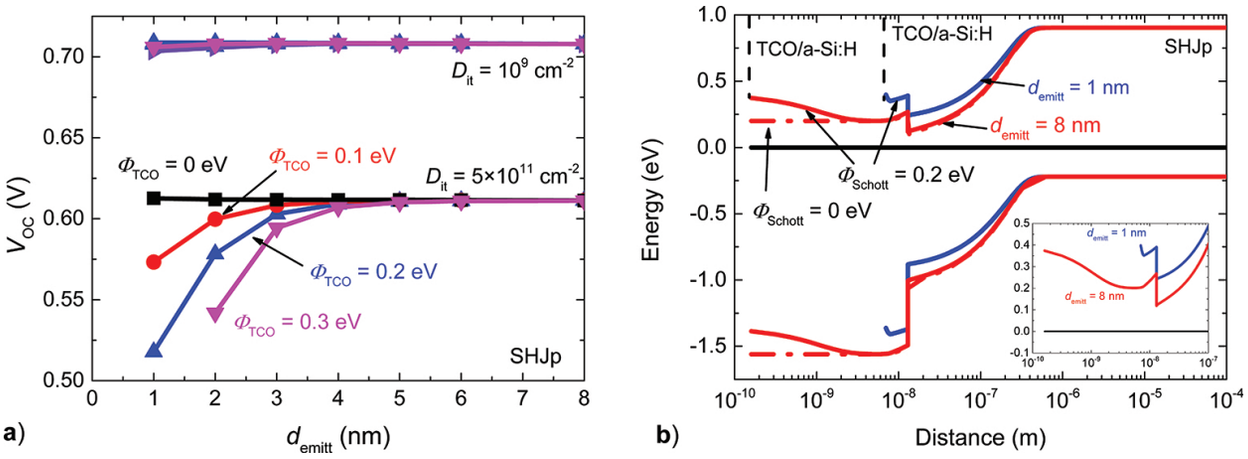

Figure 6. (a) V_{OC} calculated as a function of d_{emitt} of SHJp solar cell structure. Φ_{TCO} is varied as a parameter and two values of D_{it} are used in the simulations. (b) Band diagrams calculated for two values of d_{emitt} and Φ_{TCO} = 0.2 eV for SHJp solar cell structure. The band diagrams are aligned to place the heterointerface at the same distance. The inset shows the change in the carrier inversion.

Similar effect of Φ_{TCO} is presented in SHJn structure. Comparing SHJn and SHJp structures, the main difference is in the dopation type of amorphous emitter and thus required W_f of TCO to obtain good TCO/a-Si:H contact. Due to the presence of n-type a-Si:H emitter in SHJp solar cell, the TCO lower than at least 4.5 eV is required [24]. Typically, TCO materials have W_f higher than 4.5 eV [49, 50], which make the design of SHJp more challenging and require higher thicknesses or higher doping of a-Si:H emitter layer. In case of SHJn solar cells, the minimal W_f = 5.1 eV is required to obtain good TCO/a-Si:H contact [24], resulting in the lower technological obstacles for preparation of good TCO/a-Si:H contact.

5. The role of interfaces in SHJ working under concentrated light

Recently, possible utilization of silicon-based solar cells in light concentration applications became an attractive approach to increase the energy yield from such solar cell structures [51,

52]. Thus, it is of high interest to explore possible aspects connected with the SHJ solar cells for utilizations under concentrated light. Due to the formation of heterojunctions between a-Si:H layers and the c-Si absorption layer, the carrier transport has to overcome barriers at the front and back interfaces of the SHJ structure. Such barriers can significantly affect the collection of photo-generated carriers and thus the solar cell performance at high light intensity. Moreover, the increased light intensity absorbed by the solar cell represents a considerable amount of energy which is partially transformed to thermal energy and causes an increase of cell temperature. Because of this, the impact of the elevated temperature of such a solar cell is considered in the simulations as well. **Figure 7(a)** shows the efficiency as a function of concentrated light expressed in the suns (1 sun = 1000 W/m^2) calculated at 300, 340 and 380 K for both SHJn and SHJp structures. As can be seen, the efficiency at 1 sun decreases with temperature for both SHJ structures. Such decreases are due to the increase of the saturation current caused by an increase of the intrinsic carrier concentration in the c-Si. Saturation current lowers the V_{OC} (see Eq. 5), which consequently results in a decrease of efficiency. In general, the increase of light concentration causes an increase of the light generation g and excess concentration of carriers $\Delta p = \Delta n$, thus results in an increases of V_{OC} according to Eqs. (1) and (2) for SHJp and SHJn, respectively (see Section 2). Simulated results revealed that the efficiency of SHJ structures reach the maximum value at particular light concentration and then starts to decrease. With increased temperature the maximum of the efficiency is shifted to higher values of light concentrations. The temperature dependence of efficiency suggests that the source of efficiency drop at higher light concentrations is the presence of barriers for carrier transport which are partially overcome at higher temperatures by thermionic emission. Such carrier transport limitations are reflected also in FF. **Figure 7(b)** shows FF calculated as a function of light concentration for both SHJn and SHJp structures. The FF exhibits a similar trend to V_{OC}, and decreases significantly at high light concentrations. This drop is more relevant for SHJp structure. Considering the band diagrams of both SHJ structures (see **Figures 2a** and **b**), it can be suggested that different barriers are limiting carrier transport in SHJp and SHJn solar cells. In the case of SHJn, the photo-generated holes are collected through the front heterointerface and photo-generated electrons are collected through the back surface field (BSF) formed in our case by the c-Si/a-Si:H(n) contact. For SHJn structure, the valence band offset at the front a-Si:H/c-Si ΔE_V attains considerable higher values of 0.55 eV compared to the conduction band offset ΔE_C = 0.15 eV at the back BSF contact. It can be assumed that, due to the higher barrier, the front a-Si:H/c-Si heterointerface will be the main limitation factor for the transport of photo-generated carriers. In the case of SHJp structure, photo-generated electrons are collected through the front a-Si:H(n)/c-Si(p) contact, while photo-generated holes are collected through the back c-Si(p)/a-Si:H(p) BSF contact. ΔE_C for minority electrons at the front heterointerface is around 0.15 eV, while the barrier for holes ΔE_{BSF} can reach values around 0.7 eV. Because of this, it can be assumed that the back contact is the limiting factor for the carrier transport for SHJp structure.

ASA simulation was carried out to confirm the negative impact of the front ΔE_V and back ΔE_{BSF} barrier for carrier transport of SHJn and SHJp structures, respectively. **Figure 8(a)** shows the simulated efficiency as a function of light concentration for SHJn at 300 K with considered variation in ΔE_V from 0.65 to 0.45 eV. ΔE_V has a negligible impact on the efficiency at 1 sun light

concentration. With the increase of the light concentration the efficiency exhibits a decrease, which is more relevant for higher ΔE_V values. We can assume that such a decrease of efficiency is connected with limitation of carrier transport through ΔE_V barrier. **Figure 8(b)** shows the efficiency of SHJp calculated as a function of light concentration with a varied barrier for holes ΔE_{BSF}. The results show that the onset of the efficiency decrease is shifted to higher light concentrations with an increase of ΔE_{BSF}. Further simulations revealed (not shown in this chapter) that varying of the front ΔE_C has no impact on the efficiency behaviour with the change of light concentration. Such trends justify the back ΔE_{BSF} barrier to be responsible for the limitation of carrier transport and efficiency losses at high light concentrations of SHJp solar cell structure.

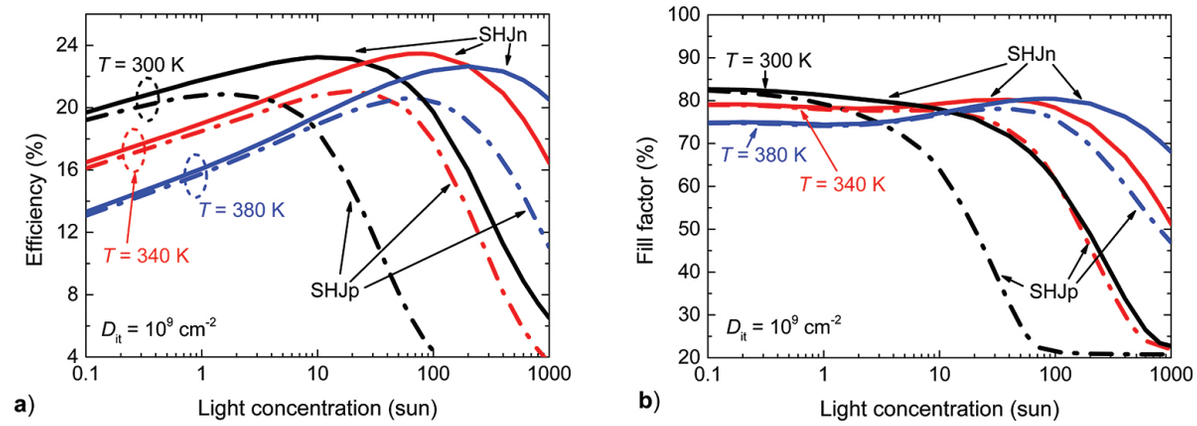

Figure 7. (a) Efficiency η and (b) FF calculated as a function of light concentration at temperatures 300, 340 and 380 K for SHJn (solid lines) and SHJp (dashed lines) structures.

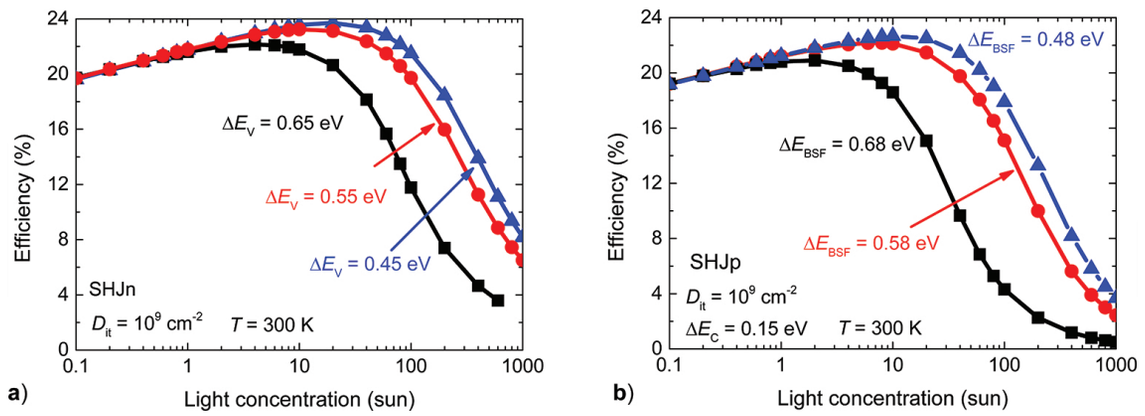

Figure 8. (a) Efficiency η calculated as a function of light concentration for different values of ΔE_V of SHJn solar cell structure. (b) Efficiency η calculated as a function of light concentration for different values of ΔE_{BSF} of SHJp solar cell structure.

From the above discussion it is clear that the presence of barriers for carrier transports has to be taken into account when the SHJ is designed for light concentration applications. While amorphous silicon forms higher ΔE_V than ΔE_C with c-Si, the barriers for collections of holes

are the main source of carrier transport limitations. In the case of SHJn structure such a barrier is formed at the front a-Si:H/c-Si interface while for SHJp structure this barrier is placed at the back c-Si/a-Si:H BSF contact. Due to the presence of thermionic emission causing a temperature-dependent carrier transport mechanism through such barriers, adjustment of the working temperature with light concentration has to be considered in order to attain the highest possible efficiency of SHJ solar cells in concentrated solar applications.

Our recent study shows that the higher operation temperature has a beneficial effect not only in enhancement of the carrier transport through barriers formed by the a-Si:H/c-Si interface but also decreases the negative impact of the parasitic Schottky barrier at the TCO/a-Si:H interface [53]. The negative influence of such barriers is more significant for SHJn structure, where the Schottky barrier depletes the emitter and increases the negative influence of ΔE_V. Thus, the optimization of SHJn solar cell structures for solar applications under concentrated light is more challenging compared to SHJp solar cell structures.

6. Conclusion

This chapter was devoted to a-Si:H/c-Si and TCO/a-Si:H heterointerfaces forming the front emitter stack with the aim to explain the influence of such heterointerfaces on V_{OC} and output performance of SHJp and SHJn solar cells. It was shown that the carrier inversion at the c-Si surface of a-Si:H/c-Si plays a key role for V_{OC} and the output performance. Various properties affecting the carrier inversion in the SHJ solar cells were analysed by means of numerical simulation leading to several conclusions. Low defect states at the interface as well as large band offset for minority carriers at a-Si:H/c-Si heterojunction are crucial to achieve strong carrier inversion and high V_{OC}. The insertion of an a-Si:H(i) passivation layer provides a decrease of the defect states at the interface; however, careful tuning of the passivation layer thickness is required to achieve a strong passivation effect with a negligible negative effect of the potential drop over this passivation layer. The Schottky barrier at the TCO/a-Si:H interface acts as a parasitic junction with opposite direction of the electric field to the electric of a-Si:H/c-Si junction. In the case of weak carrier inversion and small emitter thickness, the effect of the parasitic Schottky barrier is not screened by the charge in the emitter or minority carriers in the inversion layer and the Schottky barrier deteriorates the performance of SHJ solar cell. The simulation of SHJ structures at concentrated light conditions revealed a crucial effect of the barriers for hole collection on the efficiency. Tuning of such barriers together with tuning of the operation temperature is required to achieve a high performance of SHJ solar cells under concentrated light conditions. Due to the higher valence band offset compared to the conduction band offset at the a-Si:H/c-Si interface, higher carrier inversion is observed at the front heterointerface of SHJn solar cells leading to higher V_{OC} and lower sensitivity to defect states at the heterointerface for SHJn solar cells compared to SHJp solar cell. Two alternative concepts with the ability to provide high carrier inversion at the heterointerfaces were presented. The first one is based on the field effect passivation provided by insertion of a highly doped c-Si layer at the interface and the second one is based on the replacement of a-Si:H emitter by metal

oxide with high W_f, which provides favourable band alignment for formation of strong carrier inversion at the heterointerface.

Acknowledgements

This work was supported by the Scientific Grant Agency of the Ministry of Education of the Slovak Republic and of the Slovak Academy of Sciences under project VEGA 1/0651/16 and Slovak Research and Development Agency under the contract APVV-15-0152.

Author details

Miroslav Mikolášek

Address all correspondence to: miroslav.mikolasek@stuba.sk

Faculty of Electrical Engineering and Information Technology, Institute of Electronics and Photonics, Slovak University of Technology in Bratislava, Bratislava, Slovakia

References

[1] Louwen A, Van Sark W, Schropp R, Faaij A: A cost roadmap for silicon heterojunction solar cells. Sol Energy Mater Sol Cells. 2016;147:295–314. DOI: 10.1016/j.solmat.2015.12.026

[2] Sakata H, Tsunomura Y, Inoue H, Taira S, Baba T, Kanno H, et al.: R&d progress of next-generation very thin hit. In: Proceedings of 2010 25th European Photovoltaic Solar Energy Conference and Exhibition/5th World Conference on Photovoltaic Energy Conversion, 6–10 September 2010, Valencia, Spain. 2010. pp. 1102–1105.

[3] Tanaka M, Taguchi M, Marsuyama T, Sawada T, Hanafusa H, Kuwano Y: Development of new a-Si/c-Si heterojunction solar cells: ACJ-HIT (artifically constructed junction-heterojunction with intrinsic thin-layer). Jpn J Appl Phys. 1992;31:3518–3522. DOI: 1347-4065/31/11R/3518

[4] Masuko K, Shigematsu M, Hashiguchi T, Fujishima D, Kai M, Yoshimura N, et al.: Achievement of more than 25% conversion heterojunction solar cell. IEEE J Photovoltaics. 2014;4(6):1433–1435. DOI: 10.1109/JPHOTOV.2014.2352151

[5] Sawada T, Terada N, Tsuge S, Baba T, Takahama T, Wakisaka K, et al.: High-efficiency a-Si/c-Si heterojunction solar cell. Proc 1994 IEEE 1st World Conf Photovolt Energy

Convers – WCPEC (A Jt Conf PVSC, PVSEC PSEC). 1994;2:1219–1226. DOI: 10.1109/WCPEC.1994.519952

[6] Wolf S De, Descoeudres A, Holman ZC, Ballif C: High-efficiency silicon heterojunction solar cells: a review. Green. 2012;0(0):7–24. DOI: 10.1515/green-2011-0018

[7] Mishima T, Taguchi M, Sakata H, Maruyama E: Development status of high-efficiency HIT solar cells. Sol Energy Mater Sol Cells. 2011;95(1):18–21. DOI: 10.1016/j.solmat.2010.04.030

[8] Zhong CL, Luo LE, Tan HS, Geng KW: Band gap optimization of the window layer in silicon heterojunction solar cells. Sol Energy. 2014;108:570–575. DOI: 10.1016/j.solener.2014.08.010

[9] Kirner S, Mazzarella L, Korte L, Stannowski B, Rech B, Schlatmann R: Silicon heterojunction solar cells with nanocrystalline silicon oxide emitter: insights into charge carrier transport. IEEE J Photovolt. 2015;PP(99):1–5. DOI: 10.1109/JPHOTOV.2015.2479461

[10] Mazzarella L, Kirner S, Stannowski B, Korte L, Rech B, Schlatmann R: P-type microcrystalline silicon oxide emitter for silicon heterojunction solar cells allowing current densities above 40 mA/cm^2. Appl Phys Lett. 2015;106(2):023902. DOI: 10.1063/1.4905906

[11] Ruske F, Roczen M, Lee K, Wimmer M, Gall S, Hupkes J, et al.: Improved electrical transport in Al-doped zinc oxide by thermal treatment. J Appl Phys. 2010;107(1):1–8. DOI: 10.1063/1.3269721

[12] Morales-Masis M, Martin De Nicolas S, Holovsky J, De Wolf S, Ballif C: Low-temperature high-mobility amorphous IZO for silicon heterojunction solar cells. IEEE J Photovolt. 2015;5(5):1340–1347. DOI: 10.1109/JPHOTOV.2015.2450993

[13] Geissbühler J, Wolf S De, Faes A, Badel N, Jeangros Q, Tomasi A, et al.: Silicon heterojunction solar cells with copper-plated grid electrodes◎: status and comparison with silver thick-film techniques. IEEE J Photovolt. 2014;4(4):1055–1062. DOI: 10.1109/JPHOTOV.2014.2321663

[14] Bivour M, Temmler J, Steinkemper H, Hermle M: Molybdenum and tungsten oxide: high work function wide band gap contact materials for hole selective contacts of silicon solar cells. Sol Energy Mater Sol Cells. 2015;142:34–41. DOI: 10.1016/j.solmat.2015.05.031

[15] Bullock J, Cuevas A, Allen T, Battaglia C: Molybdenum oxide MoOx: a versatile hole contact for silicon solar cells. Appl Phys Lett. 2014;105(23). DOI: 10.1063/1.4903467

[16] Reddy SS, Gunasekar K, Heo JH, Im SH, Kim CS, Kim DH, et al.: Highly efficient organic hole transporting materials for perovskite and organic solar cells with long-term stability. Adv Mater. 2016;28(4):686–693. DOI: 10.1002/adma.20150372

[17] Li X, Xie F, Zhang S, Hou J, Choy WC: MoOx and V_2Ox as hole and electron transport layers through functionalized intercalation in normal and inverted organic optoelectronic devices. Light Sci Appl. 2015;4(4):e273. DOI: 10.1038/lsa.2015.46

[18] Geissbühler J, Werner J, Martin De Nicolas S, Barraud L, Hessler-Wyser A, Despeisse M, et al.: 22.5% efficient silicon heterojunction solar cell with molybdenum oxide hole collector. Appl Phys Lett. 2015;107(8): 081601. DOI: 10.1063/1.4928747

[19] Bullock J, Hettick M, Geissbühler J, Ong AJ, Allen T, Sutter-Fella CM, et al.: Efficient silicon solar cells with dopant-free asymmetric heterocontacts. Nat Energy. 2016;1:15031. DOI: 10.1038/nenergy.2015.31

[20] Balestrieri M, Pysch D, Becker JP, Hermle M, Warta W, Glunz SW: Characterization and optimization of indium tin oxide films for heterojunction solar cells. Sol Energy Mater Sol Cells. 2011;95(8):2390–2399. DOI: 10.1016/j.solmat.2011.04.012

[21] Kegel J, Angermann H, Sturzebecher U, Conrad E, Mews M, Korte L, et al.: Over 20% conversion efficiency on silicon heterojunction solar cells by IPA-free substrate texturization. Appl Surf Sci. 2014;301:56–62. DOI: 10.1016/j.apsusc.2014.01.183

[22] Mikolášek M, Racko J, Harmatha L, Gašpierik P, Šutta P: Influence of the broken symmetry of defect state distribution at the a-Si:H/c-Si interface on the performance of hetero-junction solar cells. Appl Surf Sci. 2010;256(18):5662–5666. DOI: 10.1016/j.apsusc.2010.03.023

[23] Schmidt M, Korte L, Laades A, Stangl R, Schubert C, Angermann H, et al.: Physical aspects of a-Si:H/c-Si hetero-junction solar cells. Thin Solid Films. 2007;515(19 SPEC. ISS.):7475–7480. DOI: 10.1016/j.tsf.2006.11.087

[24] Zhao L, Zhou CL, Li HL, Diao HW, Wang WJ: Role of the work function of transparent conductive oxide on the performance of amorphous/crystalline silicon heterojunction solar cells studied by computer simulation. Phys Stat Sol A. 2008;205(5):1215–1221. DOI: 10.1002/pssa.200723276

[25] Ritzau KU, Bivour M, Schroer S, Steinkemper H, Reinecke P, Wagner F, et al.: TCO work function related transport losses at the a-Si:H/TCO-contact in SHJ solar cells. Sol Energy Mater Sol Cells. 2014;131:9–13. DOI: 10.1016/j.solmat.2014.06.026

[26] Zeman M, Heuvel J van den, Kroon M, Willemen J, Pieters BE, Krč J, et al.: Advanced Semiconductor Analysis: User's Manual. 2010.

[27] Riesen Y, Stuckelberger M, Haug F-J, Ballif C, Wyrsch N: Temperature dependence of hydrogenated amorphous silicon solar cell performances. J Appl Phys. 2016;119(4): 044505. DOI: 10.1063/1.4940392

[28] Zhong C, Geng K, Luo L, Yang D: An analytical model to explore open-circuit voltage of a-Si:H/c-Si heterojunction solar cells. J Cent South Univ. 2016;23(3):598–603. DOI: 10.1007/s11771-016-3106-0

[29] Zhong CL, Yao RH, Geng KW: Characterization of interface states in a-Si:H/c-Si heterojunctions by an expression of the theoretical diffusion capacitance. J Phys D Appl Phys. 2010;43(49):495102. DOI: 10.1088/0022-3727/43/49/4951

[30] Jensen N, Rau U, Hausner R, Uppal S, Oberbeck L, Bergmann R, et al.: Recombination mechanisms in amorphous silicon/crystalline silicon heterojunction solar cells. J Appl Phys. 2000;87(5):2639–2645. DOI: 10.1063/1.372230

[31] Gudovskikh AS, Ibrahim S, Kleider JP, Damon-Lacoste J, Roca i Cabarrocas P, Veschetti Y, et al.: Determination of band offsets in a-Si:H/c-Si heterojunctions from capacitance-voltage measurements: capabilities and limits. Thin Sol Films. 2007;515(19):7481–7485. DOI: 10.1016/j.tsf.2006.11.198

[32] Maslova OA, Alvarez J, Gushina E V, Favre W, Gueunier-Farret ME, Gudovskikh AS, et al.: Observation by conductive-probe atomic force microscopy of strongly inverted surface layers at the hydrogenated amorphous silicon/crystalline silicon heterojunctions. Appl Phys Lett. 2010;97(25):10–13. DOI: 10.1063/1.3525166

[33] Schulze TF, Korte L, Ruske F, Rech B: Band lineup in amorphous/crystalline silicon heterojunctions and the impact of hydrogen microstructure and topological disorder. Phys Rev B Condens Matter Mater Phys. 2011;83(16):1–11. DOI: 10.1103/PhysRevB.83.165314

[34] Kleider JP, Gudovskikh AS, Roca I Cabarrocas P: Determination of the conduction band offset between hydrogenated amorphous silicon and crystalline silicon from surface inversion layer conductance measurements. Appl Phys Lett. 2008;92(16): 162101. DOI: 10.1063/1.2907695

[35] Essick JM, Cohen JD: Band offsets and deep defect distribution in hydrogenated amorphous silicon-crystalline silicon heterostructures. Appl Phys Lett. 1989;55(12): 1232–1234. DOI: 10.1063/1.101664

[36] Mikolášek M, Jakabovič J, Řeháček V, Harmatha L, Andok R: Capacitance analysis of the structures with the a-Si:H(i)/c-Si(p) heterojunction for solar-cell applications. J Electr Eng. 2014;65(4):254–258. DOI: 10.2478/jee-2014-0039

[37] Page MR, Iwaniczko E, Xu YQ, Roybal L, Hasoon F, Wang Q, et al.: Amorphous/crystalline silicon heterojunction solar cells with varying i-layer thickness. Thin Solid Films. 2011;519(14):4527–4530. DOI: 10.1016/j.tsf.2011.01.293

[38] Mikolášek M, Stuchlíková Ľ, Harmatha L, Vincze A, Nemec M, Racko J, et al.: Capacitance study of carrier inversion at the amorphous/crystalline silicon heterojunction passivated by different thicknesses of i-layer. Appl Surf Sci. 2014;312:152–156. DOI: 10.1016/j.apsusc.2014.03.187

[39] Carrere T, Varache R, Munoz D, Kleider JP: Insertion of a thin highly doped crystalline layer in silicon heterojunction solar cells: simulation and perspectives towards a highly efficient cell concept. J Renew Sustain Energy. 2015;7(1): 011202. DOI: 10.1063/1.4908189

[40] Mikolášek M, Príbytný P, Donoval D, Marek J, Chvála A, Molnár M, et al.: Suppression of interface recombination by buffer layer for back contacted silicon heterojunction solar cells. Appl Surf Sci. 2014;312:145–51. DOI: 10.1016/j.apsusc.2014.05.110

[41] Gerling LG, Mahato S, Morales-Vilches A, Masmitja G, Ortega P, Voz C, et al.: Transition metal oxides as hole-selective contacts in silicon heterojunctions solar cells. Sol Energy Mater Sol Cells. 2016;145:109–115. DOI: 10.1016/j.solmat.2015.08.028

[42] Carrere T, Varache R, Le Perchec J, Denis C, Munoz D, Kleider JP: Silicon Bulk issues during processing of homo-heterojunction solar cells. Energy Procedia. 2015;77:451–457. DOI: 10.1016/j.egypro.2015.07.064

[43] Meyer J, Hamwi S, Kroger M, Kowalsky W, Riedl T, Kahn A: Transition metal oxides for organic electronics: energetics, device physics and applications. Adv Mater. 2012;24(40):5408–427. DOI: 10.1002/adma.201201630

[44] Zhao L, Zhou CL, Li HL, Diao HW, Wang WJ: Design optimization of bifacial HIT solar cells on p-type silicon substrates by simulation. Sol Energy Mater Sol Cells. 2008;92(6): 673–681. DOI: 10.1016/j.solmat.2008.01.018

[45] Bivour M, Schröer S, Hermle M: Numerical analysis of electrical TCO/a-Si:H(p) contact properties for silicon heterojunction solar cells. Energy Procedia. 2013;38:658–669. DOI: 10.1016/j.egypro.2013.07.330

[46] Kirner S, Hartig M, Mazzarella L, Korte L, Frijnts T, Scherg-Kurmes H, et al.: The Influence of ITO dopant density on J-V characteristics of silicon heterojunction solar cells: experiments and simulations. Energy Procedia. 2015;77(1):725–732. DOI: 10.1016/j.egypro.2015.07.103

[47] Klein A, Körber C, Wachau A, Säuberlich F, Gassenbauer Y, Harvey SP, et al.: Transparent conducting oxides for photovoltaics: manipulation of fermi level, work function and energy band alignment. Materials (Basel). 2010;3(11):4892–4914. DOI: 10.3390/ma3114892

[48] Centurioni E, Iencinella D.: Role of front contact work function on amorphous silicon/crystalline silicon heterojunction solar cell performance. IEEE Electron Device Lett. 2003;24(3):177–179. DOI: 10.1109/LED.2003.811405

[49] Minami T, Miyata T, Yamamoto T.: Work function of transparent conducting multicomponent oxide thin films prepared by magnetron sputtering. Surf Coat Technol. 1998;108-109:583–587. DOI: 10.1016/S0257-8972(98)00592-1

[50] Kim JS, Lägel B, Moons E, Johansson N, Baikie ID, Salaneck WR, et al.: Kelvin probe and ultraviolet photoemission measurements of indium tin oxide work function: a comparison. Synth Met. 2000;111:311–314. DOI: 10.1016/S0379-6779(99)00354-9

[51] Descoeudres A, Allebé C, Badel N, Barraud L, Jonathan Champliaud, Debrot F, et al.: Silicon heterojunction solar cells: towards low-cost high-efficiency industrial devices and application to low-concentration PV. Energy Procedia. 2015;77:508–514. DOI: 10.1016/j.egypro.2015.07.072

[52] Paternoster G, Zanuccoli M, Bellutti P, Ferrario L, Ficorella F, Fiegna C, et al.: Fabrication, characterization and modeling of a silicon solar cell optimized for concentrated

photovoltaic applications. Sol Energy Mater Sol Cells. 2015;134:407–416. DOI: 10.1016/j.solmat.2014.12.026

[53] Mikolášek M, Racko J, Harmatha L.: Analysis of low temperature output parameters for investigation ofsilicon heterojunction solar cells. Appl Surf Sci. 2016; DOI: 10.1016/j.apsusc.2016.04.023

IntechOpen